Changes in damaging hail in major Australian cities with global warming

Timothy H. Raupach[1,2,3], **Joanna Aldridge**[4,5]

[1]UNSW Institute for Climate Risk and Response, UNSW Sydney, New South Wales, Australia
[2]UNSW Climate Change Research Centre, UNSW Sydney, New South Wales, Australia
[3]ARC Centre of Excellence for Climate Extremes, Sydney, New South Wales, Australia
[4]School of Geosciences, University of Sydney, Sydney, New South Wales, Australia
[5]QBE Australia, Sydney, New South Wales, Australia

Key Points:

- Hail causes more damage when hailstones are larger or coincident winds are stronger, yet there is high uncertainty on changes in these factors with global warming.
- Convection-permitting downscaled simulations were used to investigate possible future changes in hail size and coincident wind strength over major Australian cities and the remote Goldfields region.
- The projections indicate increases in hailstorm severity in areas around the major population centers of Melbourne, Canberra and Sydney, with increased windblown hail risk in the remote Goldfields region, and non-significant changes in other studied domains.

Corresponding author: Timothy H. Raupach, `timothy.h.raupach@gmail.com`

Abstract

In Australia, hailstorms are a leading cause of insured losses, with damage exacerbated if hailstones are large or there are coincident strong winds. Despite the high damage potential of such storms, changes to their frequency and severity under global warming are not well understood. Here, we use downscaled simulations over major cities and a remote region in Australia to project changes in hail frequency, hailstone size, and coincident wind speeds under a future scenario with ∼2.8 ° Celsius warming over pre-industrial global mean temperature. The study regions cover over 60% of the total Australian population. Generalized extreme value analysis was used to examine changes in daily maximum hail sizes and coincident wind speeds. The projections show higher future hail damage potential in some regions, with increases in hail frequency in the Sydney/Canberra and Brisbane regions, and robust increases in maximum hail size and coincident wind strength in the Melbourne and Sydney/Canberra regions.

Plain Language Summary

Hailstorms endanger lives and damage property, leading to large insured losses in Australia. Hailstorms are more damaging if the hailstones they produce are larger. They are also more damaging if there is high wind at the same time, because the wind can throw hailstones sideways into breakable materials such as windows or house facades. We expect climate change to affect hailstorms, but there have been few studies on how hailstorm frequency and severity may change in future in Australia. In this study we used simulations of weather in a future, warmer climate scenario to look at possible changes in hailstone size and in the strength of winds when hail occurs, over major cities and a remote area in Australia. The simulations project an increase in hail severity for the heavily populated Melbourne and Sydney/Canberra regions, an increase in hail frequency in Sydney/Canberra and Brisbane regions, and no significant changes in the other areas we studied.

1 Introduction

Hailstorms are most damaging when the hailstones they produce are larger (Brimelow et al., 2002; Eccel et al., 2012), and when there are co-occurring strong winds that throw hailstones sideways (Changnon, 1967; Towery et al., 1976). While anthropogenic climate change is expected to affect severe convective storms (Allen, 2018) and their associated hazards of hail (Raupach et al., 2021) and extreme winds (Brown & Dowdy, 2021), there remains high uncertainty and geographical heterogeneity in projections of how these changes will manifest (Raupach et al., 2021; Brown & Dowdy, 2021), and changes in the co-occurrence of hail and high winds have been virtually unstudied. Here, we use high-resolution downscaled simulations of a future, warmer environment to compare changes in hail damage potential over hail-prone areas of Australia.

(Impacts in Australia) Severe convective storms are responsible for insured losses of over $A40b in Australia from 1967 to 2023 (in 2022 dollars), accounting for 25% of insured catastrophe losses (Insurance Council of Australia, 2024). The largest insured loss for any event in Australian history, at $8.845b (normalized to 2022 dollars, Insurance Council of Australia, 2024), was caused by the April 1999 hailstorm impacting the eastern suburbs of Sydney. Canberra and Brisbane have also experienced hail events with normalized losses over AUD $1b (Insurance Council of Australia, 2024) **(check ref)**.

(Reasons for combining hail and wind) Hail and convective winds are often studied separately, with typical severe convective storm catastrophe models generating synthetic event sets of hail and wind hazards as separate event footprints **(ref)**. However, the coincidence of wind and hail is an important driver of loss. Wind-driven hail, both due to its greater force and oblique angle of impact, has greater potential to injure people, destroy crops (Changnon, 1967; Towery et al., 1976) and cause damage to the built environment,

such as damaging cladding to external walls, smashing windows of buildings and motor vehicles and letting rainwater inside to damage internal fixtures and contents **(ref)**. Examination of recent high-loss hail events in Australia shows that wind is often mentioned as a contributing factor **(ref)**. Common thresholds for damaging conditions include hail over 2 cm **(ref)** or wind gusts over 90 km h^{-1} (Allen, 2018). Wind driven hail events are defined as hail exceeding 5 cm and wind gusts exceeding 100 km/h (27.8 m/s) occurring in the same system within a one-hour timeframe **(ref)**. Wind driven hail events are most likely to be associated with supercells where downbursts occur **(ref)**. Observational data in the United States of America (USA) identified squall lines, isolated cells, and clusters of cells as the most frequent systems associated with wind driven hail (Carletta, 2010). (Bell et al., 2023) compiled 1646 hail and wind damage swaths for the mid-west of the USA using satellite observations for use in future understanding of the frequency of these events.

(What is known of hail and wind changes with global warming) (Allen et al., 2014) used an environment-based approach to suggest an increase in severe thunderstorm incidence in south-east Australia, although with a wide range of uncertainty. (Walsh et al., 2016) review the current and future storm-related wind and hail hazard in Australia and found future projections of wind hazard increase along the populated east coast of Australia. **(More to add here.)**

(Australian context re building codes) While wind loadings are currently considered in the Australian building code (Australian Building Codes Board, 2024) under standard AS1170.2 (Standards Australia, 2021), the impact of hail and wind-driven hail is not currently considered in Australian building design. The Association of Consulting Structural Engineers (2022) discuss hail loading on roofs and acknowledge that this effect is not accounted for under the current design standards. The April 2015 hail event impacting western Sydney is discussed including the collapse of warehouse buildings from hail loading on roofs. A guide of ultimate limit and service limit state designs for various building types is presented, but wind driven hail is not considered. Some roofing products are tested for hail impacts against standards, but many products are unrated. In ICC building code (International Code Council, 2008), hail is considered in two hail regions in the USA defined using observational data: moderate and severe, depending on the likelihood of at least one day of 1.5–3 mm **(check)** hail in a 20-year period. This code requires testing of roofing materials such as asphalt, wood and slate shingle, clay or concrete tiles, metal roofing panels and shingles in these zones. The changing occurrence of hail over time is not considered. In Canada, while hail impact is not considered in the current building code, although change is being sought in the aftermath of the 2020 Calgary hailstorm which caused $C1.4b of insured loss. Resilience measures may include increasing roof slope, using resistant roofing materials and roof underlays (Institute for Catastrophic Loss Reduction, 2018). They found that a steeper roof limits damage from wind-driven hail on the leeward side. The lack of research into impact resistant non-roof housing elements, such as windows, doors, sidings, fascia and skylights, is noted, and these elements are often subject to damage in the most destructive storms.

(What we have done here) Here, we seek to understand how the coincidence of extreme winds and damaging hail may change in a future climate in Australia. We considered analyses covering the major Australian cities of Perth, Adelaide, Melbourne, Canberra, Sydney, and Brisbane, and a remote region around the town of Kalgoorlie in the Western Australian Goldfields region. The populations of these cities add to over 60% of the total Australian population **(ref)**. Proxy-based climatologies show these regions to be hail-prone (Raupach, Soderholm, Warren, & Sherwood, 2023).

2 Methods

2.1 Simulations of historical and projected weather

Historical and future simulations were produced using the Advanced Research Weather Research and Forecasting (AR-WRF) weather model version 4.4.1 (Skamarock et al., 2021) for six nested domains. Two model configurations were used, with settings other than the domain configurations the same for both (Supporting Information Table S1). In total, we used two coarse- (∼27 km grid spacing), four medium- (∼9 km), and six fine-resolution (∼3 km) domains with a parent-child scaling ratio of three (Supporting Information Figure S1). WRF-HAILCAST (Adams-Selin et al., 2019) was enabled for the fine-resolution domains, to estimate maximum hailstone diameters at the surface. Boundary condition inputs were prepared using the `nc2wrf` code of Xu et al. (2021a).

Simulations were run for two epochs of 20 convective seasons each: the historical epoch ran from 1989 to 2009, and the future epoch from 2080 to 2100. For each convective season, simulations were run from 00Z September 30 to 18Z February 28, with hourly output resolution. Outputs were converted to local summer time and subset to cover October 1 to February 28 inclusive in each season. For each season the 14 to 16 simulated hours on 30 September local time were discarded as model spin-up time. Model outputs provide instantaneous hourly values for most variables, including wind speed at 10 m. In contrast, for each grid point and each hour, HAILCAST output the maximum hail diameter over all model time steps during the previous hour. The time step for the coarse domain was set to 100 s, but reduced to 80 s or 60 s for simulation days on which Courant-Friedrichs-Lewy (CFL) errors occurred. HAILCAST was run at every model time step, so on those days for which the time step was reduced, HAILCAST ran more often. However, here we use maximum hail sizes per day, and the sample of hail sizes per day is large, so we expect minimal effect of this time step variability. Except for the overall maxima shown in Section 4.1, we subset all our analyses to consider only times and locations where there was non-zero surface hail recorded in the preceding hour. Wind speeds and convective ingredients are thus instantaneous values in temporal proximity to hail occurrences.

2.2 Processing of simulation outputs

Examination of maximum hail size fields showed that HAILCAST occasionally produced unreasonably large hail sizes, particularly over water bodies (Supporting Information Figure S2). Since our focus is on hail hazard on land, we subset the data to land areas using the WRF land mask with small holes filled and a slight erosion applied so that points over the ocean, large bodies of water, or directly over the coastal boundary are not considered in this study. Further, we removed from consideration any HAILCAST value of surface hail over 180 mm diameter (this value being greater than the largest hail ever observed in Australia, at ∼16 cm, Australian Bureau of Meteorology, 2021). HAILCAST has been updated in more recent versions of WRF than used here, and while the updated version reduces the occurrence of unrealistically large hail sizes the changes do not affect the majority of HAILCAST results, meaning that removing very large hail sizes, as we do here, leaves a reasonable dataset for analysis (pers. comm. B. Adams-Selin, 2024). In all, less than 0.006% of non-zero hail-diameter values (not over water) were removed for being too large, per domain. Convective parameters were calculated as described in Raupach, Soderholm, Protat, and Sherwood (2023).

2.3 Statistical modelling of extreme values

Extreme value analysis was completed using the R (R Core Team, 2023) package `extRemes` (Gilleland & Katz, 2016). Block maxima were defined as daily maximum hailstone sizes and wind speeds at hail locations per domain, under the assumption that such time series can be considered independent (Coles, 2001) because single hail storms do not

last more than one day. Generalized extreme value (GEV) distributions were fitted to each series of block maxima. We used quantile-quantile (QQ) plots (Coles, 2001) and the Kolmogorov–Smirnoff (KS) test to assess the goodness of fit of the GEV distributions, by examining the similarity of the empirical distributions of block maxima and values drawn from the fitted GEV distributions. The KS test was also used to examine the (dis)similarity of GEV distributions fitted to historical versus future epochs. When the KS test was used, we generated a probabilistic view of the similarity between distributions by drawing 1000 values from the GEV distribution(s), applying the KS test, and repeating this process 100 times to generate 100 KS test results.

3 Data

Boundary conditions used for the simulations were bias-corrected data for downscaling by Xu et al. (2021b). These boundary conditions have a mean climate and interannual variance derived from European Centre for Medium-Range Weather Forecasts Reanalysis 5 (ERA5, Hersbach et al., 2020), with a non-linear trend derived from the ensemble mean of 18 Coupled Model Intercomparison Project Phase 6 (CMIP6, Eyring et al., 2016) models (Xu et al., 2021b). Future projections used the "middle-of-the-road" SSP2-4.5 shared socioeconomic pathway (SSP, O'Neill et al., 2017). On average the historical period in our simulations (1989–2019) had a global mean temperature 0.39 K over pre-industrial temperatures (1850–1990, using the CMIP6 35-model ensemble, Gutiérrez et al., 2021) while the future period (2080–2099) had a global mean temperature 2.81 K over pre-industrial temperatures. The historical and future epochs were thus separated by 2.42 K of warming.

4 Results

4.1 Overall maxima

Before taking a more rigorous statistical approach, it is useful to consider the maps of overall maxima for the quantities of interest here: hailstone size, and 10 m wind speed at hail hours. Figure 1 shows overall maximum hail sizes across each domain for each epoch. Hailstorm tracks are visible. By eye, an increase in maximum hail sizes is apparent for domains other than Perth and Brisbane, with increases in storm coverage or activity in the Adelaide, Goldfields (Kalgoorlie), Melbourne and Canberra/Sydney domains. Maximum wind speeds at hail hours are more widespread in the future scenarios than the historic scenarios, with an eastward expansion in areas experiencing maximum wind speeds in the Brisbane and Adelaide domains and a southern shift in the Goldfields (Kalgoorlie) region (Supporting Information Figure S3).

4.2 Changes in frequency of hail

Table 1 shows changes in the frequency of hail days across the six study domains. There are significant increases in hail frequency in the Sydney/Canberra and Brisbane domains, with a 29% increase in seasonal hail days in the Sydney/Canberra region. There are small non-significant frequency decreases in Adelaide, the Goldfields (Kalgoorlie) and Melbourne domains, and an indication of an increase in seasonal hail days in the Perth region, albeit not statistically significant. The variability in seasonal hail days is similar between epochs.

4.3 Extreme value analysis

4.3.1 GEV goodness of fit

GEV models were fitted to time series of daily maximum hail sizes and 10 m wind speeds at hail hours (Supporting Information Figures S4 and S5). QQ plots for hail size show acceptable agreement with some model overestimation of high quantiles (Supporting Information Figure S6), while QQ plots for wind speed at hail hours show excellent agree-

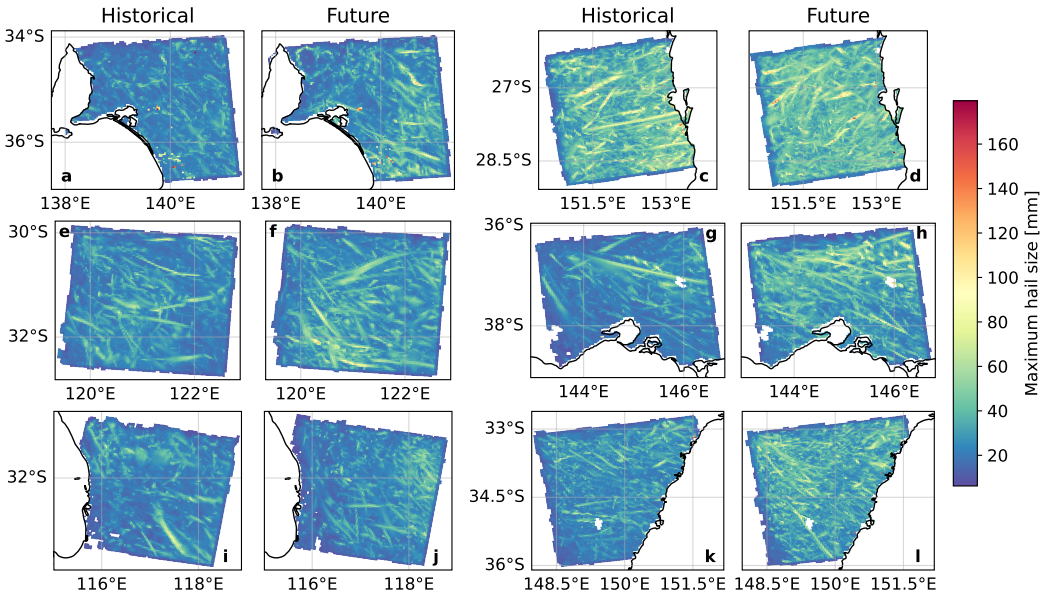

Figure 1. Maximum hail sizes in historical and future climates, for Adelaide (a, b), Brisbane (c, d), Goldfields (Kalgoorlie) (e, f), Melbourne (g, h), Perth (i, j) and Sydney/Canberra (k, l) domains.

Table 1. Mean and standard deviation of seasonal hail days in the historic and future simulations, and relative future changes with 95% confidence interval according to Welch's two-sample t-test, per domain. Statistical significance of the change calculated by Welch's two-sample t-test is indicated by $*$ for a 90% confidence level ($p < 0.1$) and $**$ for a 95% confidence level ($p < 0.05$).

Domain	Historic days	Future days		Future change
Adelaide	8.7 ± 4.2	8.35 ± 4.9	-4%	(-38% to 30%)
Brisbane	32.95 ± 8.3	37.8 ± 8.8	15%$*$	(-2% to 31%)
Kalgoorlie	10 ± 6	9.8 ± 5.2	-2%	(-38% to 34%)
Melbourne	11.7 ± 5.9	11.5 ± 7.1	-2%	(-37% to 34%)
Perth	6.8 ± 4.9	7.55 ± 4.9	11%	(-35% to 57%)
Sydney/Canberra	24.3 ± 9.4	31.4 ± 9	29%$**$	(5% to 53%)

ment between modelled and empirical quantiles (Supporting Information Figure S7). In all cases where the model was compared to empirical values, either all or the bulk of KS test p values were above the 0.05 level, indicating that the null hypothesis that the two samples are drawn from the same distribution can not be rejected (Supporting Material Figure S8). The QQ plot and KS test results show that the GEV models have sufficient goodness of fit for the analyses here.

4.3.2 Significance of changes

Having determined that the GEV fits to empirical data are valid, we now consider whether the fitted models show any significant difference between the historical and future epochs. Figure 2 shows the fitted parameters and their confidence intervals for all the GEV models used in this study. The models fitted for the Melbourne and Sydney/Canberra domains both show significant differences between epochs in the location or scale parameters

for both hail size and wind at hail hours, whereas the models for the other domains have parameters with overlapping confidence intervals. These results are further supported by the p value distributions from KS tests when historical models are compared to future models (Supporting Information Figure S8). The null hypothesis that the samples are drawn from the same distribution can be rejected for the Melbourne and Sydney/Canberra domains for both maximum hail size and maximum wind speed at hail hours, and for the Perth domain for wind only. To be conservative, we conclude that the changes in maxima between epochs are significant in the Melbourne and Sydney/Canberra domains, but not significant in the other domains.

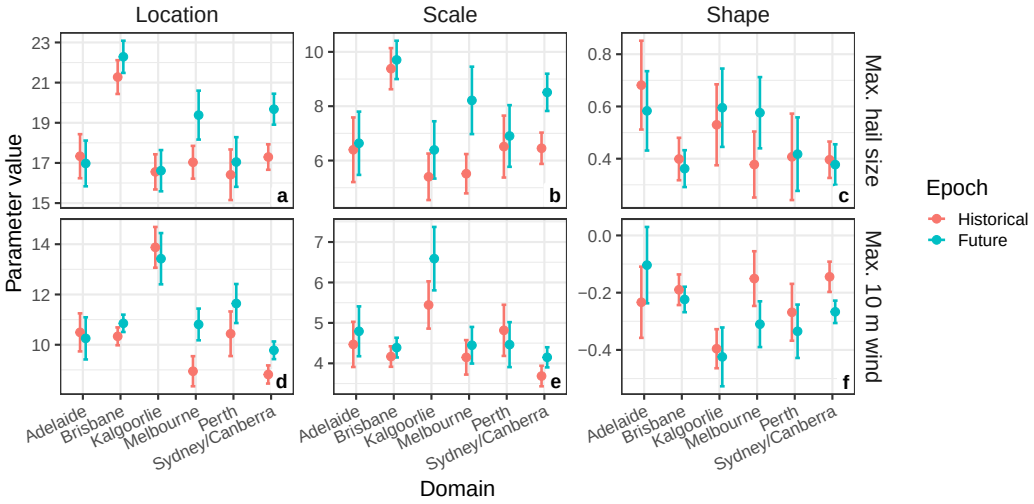

Figure 2. Location (a, d), scale (b, e), and shape (c, f) parameters for fitted GEV distributions for maximum hail size (a–c) and 10 m wind at hail hours (d–f). Parameter values are shown as a point and whiskers show 95% confidence intervals.

4.3.3 Return periods

Figure 3 shows return period curves for maximum hail size and maximum wind speed at hail hours. Because our analysis is limited to hail days, the return periods are in number of hail days, not overall days. It is not uncommon for return period models based on the GEV family to produce non-physical extreme values such as the extremely large hail sizes predicted for large return periods here (Coles, 2001, p. 66). We take the advice of Coles (2001) and interpret the results here based on the shorter return periods, thus keeping physical principles in mind. In Melbourne and Sydney/Canberra, the two domains with significant changes, there are increases in the maximum expected hail size for return periods longer than about three hail days, with the largest increase in the Melbourne region where the return period for 100 mm hail is reduced from more than 100 hail days to about 30 hail days. In both domains with significant changes the return period for lighter winds (less than about 18 m s^{-1}) is markedly shorter in the future scenario, but the return period for very strong winds is longer in the warmer scenario. For the other domains, with non-significant differences in GEV distributions, the most notable changes are a decrease in strong wind return periods for Adelaide and Goldfields (Kalgoorlie) regions and light wind return periods in the Perth region.

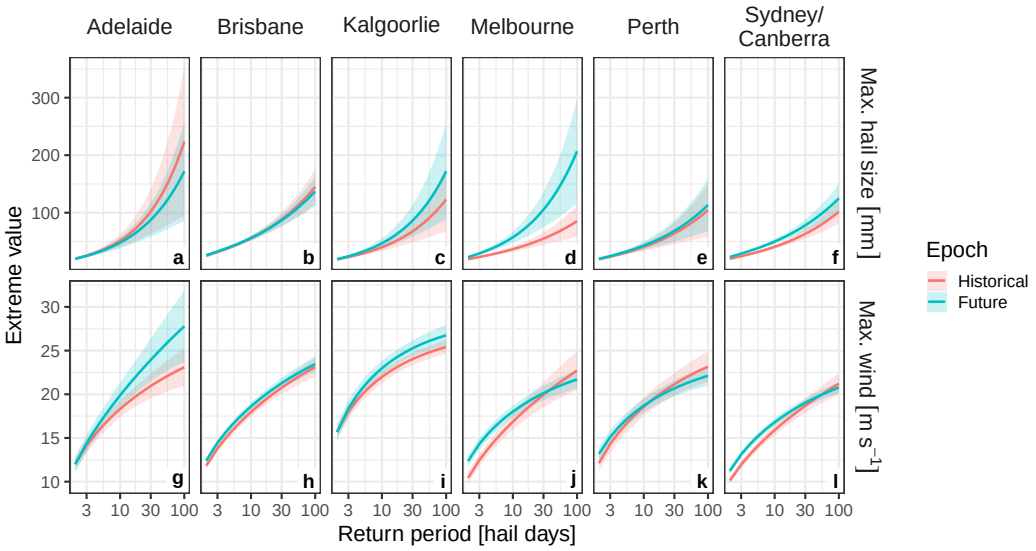

Figure 3. Return period plots for maximum hail size (a–f) and maximum wind at hail hours (g–l) for the domains of Adelaide (a, g), Brisbane (b, h), Goldfields (Kalgoorlie) (c, i), Melbourne (d, j), Perth (e, k), and Sydney/Canberra (f, l).

4.3.4 Probability of exceeding damaging thresholds

Figure 4 shows the probability of a hail day producing various damaging hail and wind thresholds at hail hours (numerical results are shown in Supporting Information Table S2), comparing historical to future epochs. For hail, we examine the probability of a hail day producing severe (20 mm), giant (50 mm), and 100 mm hail, while for wind we examine 80 and 100 km h^{-1} as damaging thresholds. In the Melbourne domain for any given hail day, the probability of severe hail jumps from ∼46% in the historical epoch to ∼61% in the future scenario, while giant hail probability roughly triples (from ∼4% to ∼13%), and 100 mm hail is more than 5 times more likely (from ∼1% to ∼4%) in the future epoch. In the Sydney/Canberra domain, any given hail day has a probability of severe hail of ∼49% in the historical epoch which increases to ∼62% in the future scenario, while giant hail probability (∼6% to ∼10%) and 100 mm hail probability (∼1% to ∼2%) both come close to doubling in the future epoch. Other non-significant increases in severe hail probability are shown for Brisbane, Perth, and Goldfields (Kalgoorlie) areas, with non-significant decreases in the Adelaide region, and the Goldfields region shows a non-significant increase also for giant hail probability. In Melbourne and Sydney/Canberra, the domains with significant differences, the probability of damaging winds at hail hours on a hail day decreases by about half for 80 km h^{-1} wind speed at hail hours. Non-significant changes include an increase in the probability of 80 km h^{-1} wind speed at hail hours in the Goldfields (Kalgoorlie) region (from ∼9% to ∼13%) and Adelaide domain (from ∼2% to ∼5%), and for 100 km h^{-1} winds at hail hours for the Adelaide region (from ∼0% to ∼1%). Other than for Adelaide, the probability of hail days producing 100 km h^{-1} wind speed at hail hours is close to zero in all domains across both epochs.

4.4 Changes in relevant atmospheric properties

Table 2 shows projected changes in daily mean hail size, wind speed, and storm-relevant atmospheric properties, at hail times, in the future compared to historical simulations. Unlike in the extreme value analysis above, here we used mean values for each season and test

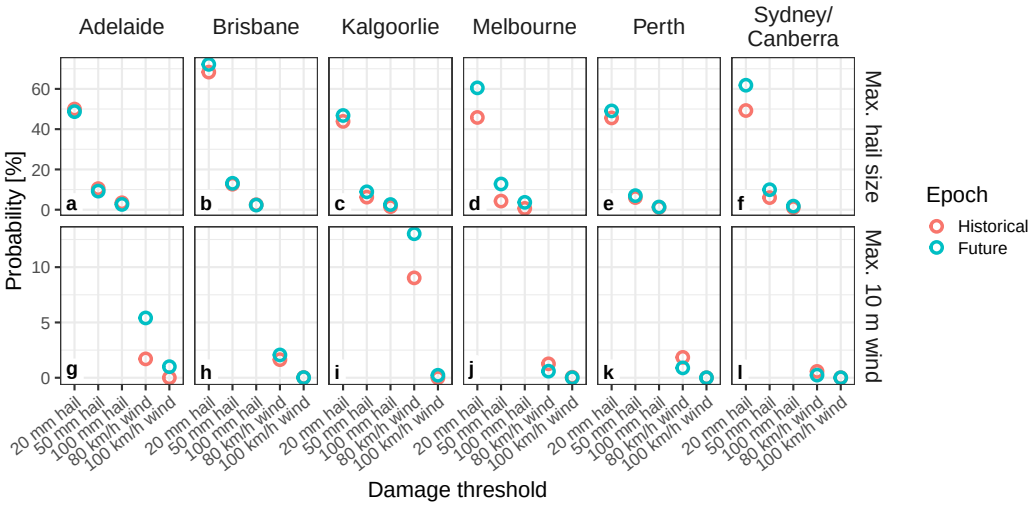

Figure 4. Changes in the probability of exceeding thresholds on hail size (a–f), and 10 m wind speed at hail hours (g–l), on any given hail day, for the domains of Adelaide (a, g), Brisbane (b, h), Goldfields (Kalgoorlie) (c, i), Melbourne (d, j), Perth (e, k), and Sydney/Canberra (f, l).

for differences between epochs using Welch's t-test. Mean hail size shows statistically significant increases in Melbourne and Sydney/Canberra, aligning with the extreme value analysis results for maximum hail size, but here there is also a significant increase in the Brisbane domain. Changes in mean wind are generally small, with the only significant changes being increases in the Perth and Sydney/Canberra domains. Changes in wind shear are varied, with a small significant increase in Kalgoorlie and a small significant decrease in Brisbane. Increases of ∼1% in temperature at 500 hPa, and 8-10% in freezing-level and melting-level heights are significant in every domain. Atmospheric instability increases in all domains, with significant increases in convective available potential energy (CAPE) at hail times in Adelaide, Brisbane, Melbourne, and Sydney/Canberra regions, while the results for lifted index (LI) are more mixed with fewer significant changes. Convective inhibition (CIN) also became stronger in all domains with significant decreases in Adelaide, Brisbane, the Goldfields (Kalgoorlie), Melbourne, and Sydney/Canberra. Lapse rate changes are generally small, although significant increases are shown in Brisbane and Sydney/Canberra. The extreme value analysis results for the domains where they showed significant changes, Melbourne and Sydney/Canberra, are supported by the large increases in convective instability and convective inhibition and freezing level height, that would support storm development, strong updrafts, and survival of large hailstones to the surface. Wind shear changes are not significant, indicating that these changes in damage are driven more by changes in instability than shear. In the Brisbane domain there is more of a balance between modest yet significant increases in instability and decreases in wind shear, indicating that in this domain there may be more offsetting of these two environmental factors leading to no significant change in damage potential in the GEV analyses.

4.5 Correlations between regions

Correlations between seasonal values of hail relevant properties are shown in Figure 5. There is co-fluctuation in hail days between the east-coast cities of Melbourne, Sydney/Canberra and Brisbane in both historical and future epochs, with Adelaide significantly correlated with Melbourne and Sydney/Canberra in the future projections. Correlations in hail diameter between the domains around Kalgoorlie, Perth, Melbourne, and

Table 2. Projected relative changes in mean hail size, 10 m wind (Wind), bulk vertical wind shear from 0-6 km (S06), convective available potential energy (CAPE), convective inhibition (CIN), lifted index (LI), temperature at 500 hPa (T500), lapse rate from 700 to 500 hPa (LR), freezing-level height (FLH), and melting-level height (MLH), for hail times by domain. Statistical significance of the difference between historical and future seasonal mean values, calculated using Welch's two-sample t-test, is shown by $*$ for the 90% confidence level, $**$ for the 95% confidence level, and $***$ for the 99% confidence level. Bracketed ranges show the 95% confidence interval on the changes. Means are daily means of variables at hail times and locations.

	Adelaide		Brisbane		Kalgoorlie	
Hail size	0%	(-4% to 3%)	4%***	(2% to 5%)	0%	(-3% to 4%)
Wind	-1%	(-7% to 5%)	2%	(-1% to 4%)	-2%	(-7% to 3%)
S06	-1%	(-9% to 7%)	-4%**	(-7% to 0%)	5%*	(-1% to 11%)
CAPE	23%*	(-2% to 49%)	9%**	(2% to 15%)	11%	(-8% to 29%)
LI	-41%	(-146% to 65%)	-8%**	(-16% to 0%)	77%*	(-7% to 161%)
CIN	-22%**	(-40% to -4%)	-8%***	(-14% to -2%)	-13%**	(-25% to -1%)
LR	-1%	(-3% to 1%)	2%***	(1% to 3%)	-1%	(-2% to 1%)
T500	1%***	(1% to 1%)	1%***	(1% to 1%)	1%***	(1% to 1%)
FLH	9%***	(7% to 11%)	9%***	(8% to 10%)	9%***	(6% to 11%)
MLH	8%***	(6% to 10%)	9%***	(8% to 10%)	9%***	(6% to 11%)
	Melbourne		Perth		Sydney/Canberra	
Hail size	4%**	(1% to 7%)	1%	(-3% to 6%)	4%***	(2% to 6%)
Wind	3%	(-2% to 8%)	9%***	(3% to 15%)	3%*	(0% to 6%)
S06	6%	(-2% to 13%)	-2%	(-10% to 6%)	-1%	(-6% to 3%)
CAPE	29%***	(14% to 44%)	14%	(-11% to 38%)	25%***	(16% to 34%)
LI	-13%	(-77% to 50%)	12%	(-72% to 96%)	-21%	(-48% to 6%)
CIN	-23%***	(-36% to -10%)	-7%	(-21% to 6%)	-15%***	(-23% to -7%)
LR	1%	(0% to 3%)	1%	(-2% to 3%)	2%***	(1% to 3%)
T500	1%***	(1% to 1%)	1%***	(0% to 1%)	1%***	(1% to 1%)
FLH	10%***	(8% to 12%)	8%***	(4% to 11%)	9%***	(8% to 10%)
MLH	10%***	(8% to 12%)	7%***	(4% to 10%)	9%***	(7% to 10%)

Sydney/Canberra are considerably stronger in the future projections that in the historical epoch, while wind correlations between the Perth region and other south-western domains of Adelaide and Kalgoorlie are evident in the historical epoch but disappear in the future projections. Instability is correlated between Melbourne and Sydney/Canberra domains in both epochs. Temperature-related values show strong correlations between nearby domains, such as the western domains of the Goldfields (Kalgoorlie) and Perth, which increase in strength in the projections, and the eastern domains of Brisbane and Sydney/Canberra.

5 Conclusions

In this study we used downscaled regional analyses to project changes in hail diameter and co-occurring wind speeds in warmer conditions, over hail-prone regions of Australia. The domains covered more than 60% of Australia's population, including the major cities of Perth, Adelaide, Melbourne, Canberra, Sydney, and Brisbane. The results show projected increases in hail frequency around Sydney/Canberra and Brisbane, projected increases in hail size around Sydney/Canberra and Melbourne, and indications of increased wind at hail hours in Adelaide and the remote Goldfields region but decreased probability of damaging wind at hail hours in Melbourne, Perth, and Sydney/Canberra. An analysis of the changes

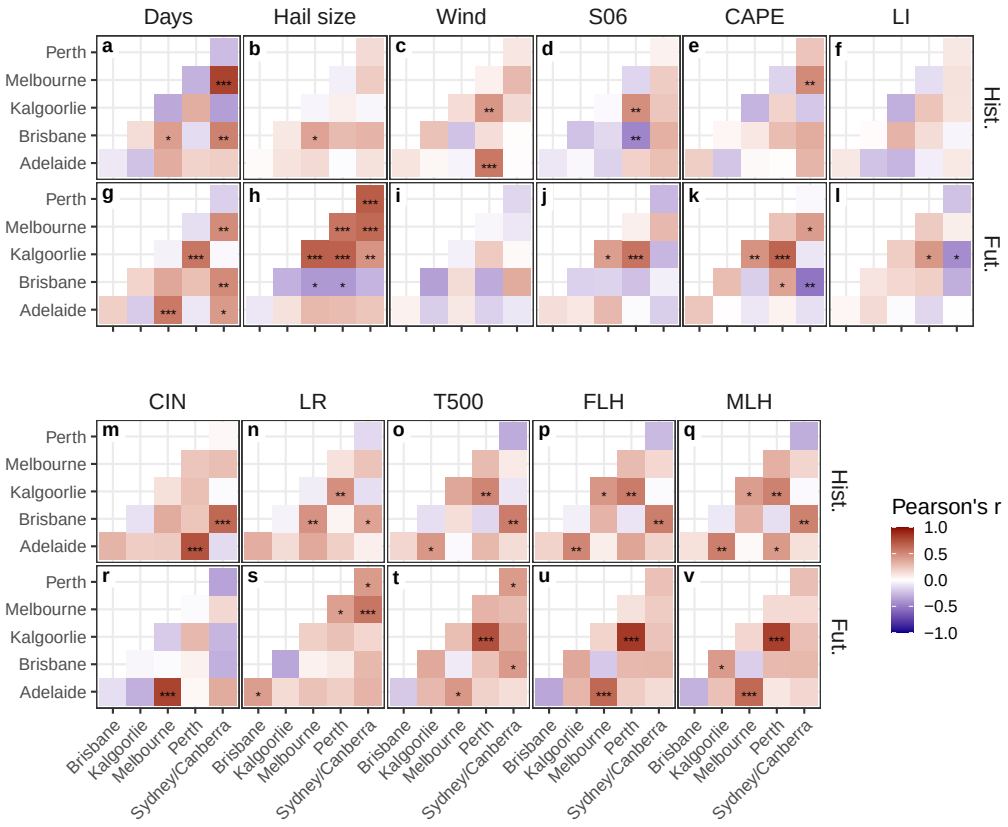

Figure 5. Correlations of seasonal values of hail-relevant properties between domains, by epoch. Seasonal means were calculated from daily means at hail locations and hours. Variables considered are seasonal hail days (a, g), and mean hail diameter (b, h), 10 m wind at hail hours (c, i), bulk vertical wind shear (d, j), CAPE (e, k), lifted index (f, l), CIN (m, r), 700-500 hPa lapse rate (n, s), temperature at 500 hPa (o, t), freezing level height (p, u) and melting level height (q, v), for historical (a-f, m-q) and future (g-l, r-v) epochs. Statistically significant correlations are shown by an $*$ for 90% confidence level ($p < 0.1$), $**$ for 95% confidence level ($p < 0.05$), and $***$ for the 99% confidence level ($p < 0.01$).

in mean atmospheric conditions at hail hours shows projected increases in atmospheric instability and freezing level height, and little change in bulk vertical wind shear in the warmer scenario. Correlations in seasonal average hail size between regions are stronger in the future than present scenario.

Several caveats apply to the results shown here. The most notable is that maximum hail sizes reported at each hour are maximums over the last hour, while wind speeds are instantaneous values within the temporal vicinity of hail occurrence. Maximum wind gusts over the previous hour would generally be significantly stronger than these instantaneous values. We also caution that these results are one realization of possible future projections, based on the boundary conditions and modelling framework used, and more ensemble members using different setups are required to build a more complete picture of possible future hazards.

Open Research Section

Boundary condition data are available at Xu et al. (2021a). Complete analysis code and WRF configuration files are available in a **(Zenodo repository)**. Convective parameters were calculated using `xarray_parcel` (DOI: 10.5281/zenodo.8088497).

Acknowledgments

Since March 2024, THR's position at UNSW Sydney has been supported by QBE Insurance. This research was undertaken with the assistance of resources from the National Computational Infrastructure (NCI Australia), an NCRIS enabled capability supported by the Australian Government. We thank Simon Tett for useful discussions on extreme value techniques.

References

Adams-Selin, R. D., Clark, A. J., Melick, C. J., Dembek, S. R., Jirak, I. L., & Ziegler, C. L. (2019). Evolution of WRF-HAILCAST during the 2014–16 NOAA/Hazardous Weather Testbed spring forecasting experiments. *Weather Forecast*, *34*(1), 61-79. doi: 10.1175/waf-d-18-0024.1

Allen, J. T. (2018, 07). *Climate change and severe thunderstorms.* Oxford University Press. doi: 10.1093/acrefore/9780190228620.013.62

Allen, J. T., Karoly, D. J., & Walsh, K. J. (2014). Future Australian severe thunderstorm environments. Part II: The influence of a strongly warming climate on convective environments. *J Climate*, *27*(10), 3848-3868. doi: 10.1175/JCLI-D-13-00426.1

Association of Consulting Structural Engineers. (2022). *Hail loading on roofs. Practice note number 19 version 2.* Retrieved from `https://www.acse.org.au/wp-content/uploads/2022/03/Practice-Paper-19-Hail-Loading-REVISED-2022.pdf` (accessed 22 June 2024)

Australian Building Codes Board. (2024). *National construction code.* Retrieved from `https://ncc.abcb.gov.au` (accessed 22 July 2024)

Australian Bureau of Meteorology. (2021). *Bureau expert explains giant hail phenomenon.* Retrieved from `https://media.bom.gov.au/releases/908/bureau-expert-explains-giant-hail-phenomenon/` (Media release, accessed 31 July 2023)

Bell, J. R., Wisinski, E. F., Molthan, A. L., Schultz, C. J., Gilligan, E., & Sharp, K. G. (2023). Developing a hail and wind damage swath event database from daily MODIS true color imagery and storm reports for impact analysis and applications. *Weather Forecast*, *38*(9), 1575 - 1588. doi: 10.1175/WAF-D-22-0210.1

Brimelow, J. C., Reuter, G. W., & Poolman, E. R. (2002). Modeling maximum hail size in Alberta thunderstorms. *Weather Forecast*, *17*(5), 1048-1062. doi: 10.1175/1520-0434(2002)017⟨1048:MMHSIA⟩2.0.CO;2

Brown, A., & Dowdy, A. (2021). Severe convective wind environments and future projected changes in Australia. *J Geophys Res-Atmos*, *126*(16), e2021JD034633. (e2021JD034633 2021JD034633) doi: 10.1029/2021JD034633

Carletta, N. D. (2010). *Severe wind-driven hail events: Dependence on convective morphology and larger-scale environment* (Master's thesis, Department of Geological and Atmospheric Sciences. Iowa State University). Retrieved from `https://meteor.geol.iastate.edu/~ncarlett/portfolio/Senior_Thesis_Carletta_Final.pdf` (accessed 22 July 2024)

Changnon, S. A. (1967). Areal-temporal variations of hail intensity in Illinois. *J Appl Meteorol*, *6*(3), 536 - 541. doi: 10.1175/1520-0450(1967)006⟨0536:ATVOHI⟩2.0.CO;2

Coles, S. (2001). *An introduction to statistical modeling of extreme values* (1st ed.). Springer London. doi: 10.1007/978-1-4471-3675-0

Eccel, E., Cau, P., Riemann-Campe, K., & Biasioli, F. (2012). Quantitative hail monitoring in an alpine area: 35-year climatology and links with atmospheric variables. *Int J Climatol*, *32*(4), 503-517. doi: 10.1002/joc.2291

Eyring, V., Bony, S., Meehl, G. A., Senior, C. A., Stevens, B., Stouffer, R. J., & Taylor, K. E. (2016). Overview of the Coupled Model Intercomparison Project Phase 6 (CMIP6) experimental design and organization. *Geosci Model Dev*, *9*(5), 1937–1958. doi: 10.5194/gmd-9-1937-2016

Gilleland, E., & Katz, R. W. (2016). extRemes 2.0: An extreme value analysis package in R. *J Stat Softw*, *72*(8), 1–39. doi: 10.18637/jss.v072.i08

Gutiérrez, J., Jones, R., Narisma, G., Alves, L., Amjad, M., Gorodetskaya, I., ... Yoon, J.-H. (2021). Atlas. In V. Masson-Delmotte et al. (Eds.), *Climate change 2021: The physical science basis. Contribution of working group I to the Sixth Assessment Report of the Intergovernmental Panel on Climate Change* (p. 1927–2058). Cambridge, United Kingdom and New York, NY, USA: Cambridge University Press. doi: 10.1017/9781009157896.021

Hersbach, H., Bell, B., Berrisford, P., Hirahara, S., Horányi, A., Muñoz Sabater, J., ... Thépaut, J.-N. (2020). The ERA5 global reanalysis. *Q J Roy Meteor Soc*, *146*(730), 1999-2049. doi: 10.1002/qj.3803

Hong, S.-Y., Noh, Y., & Dudhia, J. (2006). A new vertical diffusion package with an explicit treatment of entrainment processes. *Mon Weather Rev*, *134*(9), 2318 - 2341. doi: 10.1175/MWR3199.1

Iacono, M. J., Delamere, J. S., Mlawer, E. J., Shephard, M. W., Clough, S. A., & Collins, W. D. (2008). Radiative forcing by long-lived greenhouse gases: Calculations with the AER radiative transfer models. *J Geophys Res-Atmos*, *113*(D13). doi: 10.1029/2008JD009944

Institute for Catastrophic Loss Reduction. (2018). *Protect your home from hail.* Retrieved from `https://www.iclr.org/wp-content/uploads/2021/04/ICLR_Hail-2020_E_2021.pdf` (accessed 22 July 2024)

Insurance Council of Australia. (2024). *Historical normalised catastrophes, June 2024.* Retrieved from `https://insurancecouncil.com.au/wp-content/uploads/2024/07/ICA-Historical-Normalised-Catastrophe-June-2024.xlsx` (accessed 22 July 2024)

International Code Council. (2008). *International building code - structural.* Retrieved from `https://www.iccsafe.org/cs/codes/Documents/2007-08cycle/FAA/IBC-S1-S141-P2.pdf` (accessed 22 July 2024)

Jiménez, P. A., Dudhia, J., González-Rouco, J. F., Navarro, J., Montávez, J. P., & García-Bustamante, E. (2012). A revised scheme for the WRF surface layer formulation. *Mon Weather Rev*, *140*(3), 898 - 918. doi: 10.1175/MWR-D-11-00056.1

Milbrandt, J. A., Morrison, H., II, D. T. D., & Paukert, M. (2021). A triple-moment representation of ice in the predicted particle properties (P3) microphysics scheme. *J Atmos Sci*, *78*(2), 439 - 458. doi: 10.1175/JAS-D-20-0084.1

Niu, G.-Y., Yang, Z.-L., Mitchell, K. E., Chen, F., Ek, M. B., Barlage, M., ... Xia, Y. (2011). The community Noah land surface model with multiparameterization options (Noah-MP): 1. Model description and evaluation with local-scale measurements. *J Geophys Res-Atmos*, *116*(D12). doi: 10.1029/2010JD015139

O'Neill, B. C., Kriegler, E., Ebi, K. L., Kemp-Benedict, E., Riahi, K., Rothman, D. S., ... Solecki, W. (2017). The roads ahead: Narratives for shared socioeconomic pathways describing world futures in the 21st century. *Glob Environ Change*, *42*, 169-180. doi: 10.1016/j.gloenvcha.2015.01.004

R Core Team. (2023). R: A language and environment for statistical computing [Computer software manual]. Vienna, Austria. Retrieved from `https://www.R-project.org/`

Raupach, T. H., Martius, O., Allen, J. T., Kunz, M., Lasher-Trapp, S., Mohr, S., ... Zhang, Q. (2021). The effects of climate change on hailstorms. *Nat Rev Earth Environ*, *2*(3), 213-226. doi: 10.1038/s43017-020-00133-9

Raupach, T. H., Soderholm, J., Protat, A., & Sherwood, S. C. (2023). An improved

instability–shear hail proxy for australia. *Mon Weather Rev*, *151*(2), 545-567. doi: 10.1175/MWR-D-22-0127.1

Raupach, T. H., Soderholm, J. S., Warren, R. A., & Sherwood, S. C. (2023). Changes in hail hazard across Australia: 1979-2021. *npj Clim Atmos Sci*, *6*(1), 143. doi: 10.1038/s41612-023-00454-8

Skamarock, W. C., Klemp, J. B., Dudhia, J., Gill, D. O., Liu, Z., Berner, J., ... yu Huang, X. (2021, 7 20). *A description of the advanced research WRF version 4.3* (Tech. Rep.). Boulder, Colorado, USA: National Center for Atmospheric Research. (NCAR technical note NCAR/TN-556+STR) doi: 10.5065/1dfh-6p97

Standards Australia. (2021). *AS/NZS 1170.2 structural design actions, part 2 wind actions.* Retrieved from `https://store.standards.org.au/product/as-nzs-1170-2-2021` (accessed 22 July 2024)

Towery, N. G., Morgan, G. M., & Changnon, S. A. (1976). Examples of the wind factor in crop-hail damage. *J Appl Meteorol*, *15*(10), 1116 - 1120. doi: 10.1175/1520-0450(1976)015⟨1116:EOTWFI⟩2.0.CO;2

Walsh, K., White, C. J., McInnes, K., Holmes, J., Schuster, S., Richter, H., ... Warren, R. A. (2016). Natural hazards in Australia: storms, wind and hail. *Climatic Change*, *139*(1), 55-67. doi: 10.1007/s10584-016-1737-7

Xu, Z., Han, Y., Tam, C.-Y., Yang, Z.-L., & Fu, C. (2021a, January). *Bias-corrected CMIP6 global dataset for dynamical downscaling of the Earth's historical and future climate (1979-2100).* Science Data Bank. doi: 10.11922/sciencedb.00487

Xu, Z., Han, Y., Tam, C.-Y., Yang, Z.-L., & Fu, C. (2021b). Bias-corrected CMIP6 global dataset for dynamical downscaling of the historical and future climate (1979–2100). *Sci Data*, *8*(1), 293. doi: 10.1038/s41597-021-01079-3

Zhang, C., & Wang, Y. (2017). Projected future changes of tropical cyclone activity over the Western North and South Pacific in a 20-km-mesh regional climate model. *J Climate*, *30*(15), 5923 - 5941. doi: 10.1175/JCLI-D-16-0597.1